© 2018. Published by The Company of Biologists Ltd | Journal of Experimental Biology (2018) 221, jeb191148. doi:10.1242/jeb.191148

RESEARCH ARTICLE

Jet-paddling jellies: swimming performance in the Rhizostomeae jellyfish *Catostylus mosaicus*

Thomas R. Neil* and Graham N. Askew‡

ABSTRACT

Jellyfish are a successful and diverse class of animals that swim via jet propulsion, with swimming performance and propulsive efficiency being related to the animal's feeding ecology and body morphology. The Rhizostomeae jellyfish lack tentacles but possess four oral lobes and eight trailing arms at the centre of their bell, giving them a body morphology quite unlike that of other free-swimming medusae. The implications of this body morphology on the mechanisms by which thrust is produced are unknown. Here, we determined the wake structure and propulsive efficiency in the blue-blubber jellyfish *Catostylus mosaicus* (order: Rhizostomeae). The animal is propelled during both bell contraction and bell relaxation by different thrust-generating mechanisms. During bell contraction, a jet of fluid is expelled from the subumbrellar cavity, which results from the interaction between the counter-rotating stopping (from the preceding contraction cycle) and starting vortices, creating a vortex superstructure and propulsion. This species is also able to utilise passive energy recapture, which increases the animal's swimming velocity towards the end of the bell expansion phase when the bell diameter is constant. The thrust produced during this phase is the result of the flexible bell margin manoeuvring the stopping vortex into the subumbrellar cavity during bell relaxation, enhancing its circulation, and creating a region of high pressure on the inner surface of the bell and, consequently, thrust. These mechanisms of thrust generation result in *C. mosaicus* having a relatively high propulsive efficiency compared with other swimmers, indicating that economical locomotion could be a contributing factor in the ecological success of these medusan swimmers.

KEY WORDS: Medusa, Fluid dynamics, Wake structure, Vorticity, Cnidaria, Scyphozoa

INTRODUCTION

Many free-swimming medusae swim by jet propulsion. Contraction of muscle fibres deforms the mesoglea, compressing the subumbrella cavity and forcing water out of the bell mouth, which transfers momentum to the environment. Subsequently, the bell is expanded by elastic recoil of the mesoglea. Medusae have traditionally been considered as poor locomotory performers, with swimming efficiencies much lower than that of undulatory swimmers (Dabiri et al., 2010; Gemmell et al., 2013) and unimpressive swimming speeds (Alexander, 2003). However, there is a wide variation in swimming efficiency (0.09 to 0.53; Dabiri et al., 2010) and all medusae studied to date are economical swimmers, with a metabolic cost of locomotion that is similar to or an order of magnitude lower than similarly sized fish (Gemmell et al., 2013). The variations in swimming efficiency are due to differences in the mechanics of jet propulsion, and related to the animal's feeding ecology and body morphology. It appears that there is a trade-off between swimming speed and propulsive efficiency (Dabiri et al., 2010).

Medusae of species that are ambush predators have prolate bells, and spend much of their time drifting on water currents, only swimming infrequently to escape predation and change position in the water column (Weston et al., 2009). They create wake vortex rings with trailing jets and exhibit higher relative swimming speeds but with relatively low propulsive efficiencies (Dabiri et al., 2010). Increased thrust occurs by increasing the mass of fluid entrained into the vortex ring before 'pinch-off' occurs (Dabiri and Gharib, 2004; Gharib et al., 1998). This is achieved in medusae of several species by manipulating the shape of the orifice through which water is ejected by contracting the velum during bell contraction, delaying pinch off and increasing the size of the vortex ring and increasing thrust generation. The presence of velar structures in fast-swimming jellyfish and the occurrence of similar jet-regulating mechanisms in other jet-propelled swimmers (e.g. the funnel of squid) appear to be a primary factor contributing to the success of fast-swimming jetters, despite their primitive body plans.

Cruising predatory species swim relatively slowly by the almost continuous cyclical contraction of their oblate bells, using a form of jet propulsion referred to as 'rowing'. In the medusae of these species, the wakes consist of distinct vortex rings and their propulsive efficiency is relatively high. Thrust production in this type of wake can be augmented if successive vortex rings are closely spaced (less than three vortex ring radii apart) due to the velocity induced on adjacent vortices in the wake, in comparison to an isolated vortex ring (Weihs, 1977). Flow patterns generated by jellyfish show that the interactions between stopping and starting vortices lead to reduced propagation of downstream wake vortices, resulting in close spacing between adjacent vortices and the potential for thrust augmentation (Dabiri et al., 2005). An additional energy saving mechanism has been identified in medusae with oblate bells. These species swim with a jet-paddling form of locomotion that produces a more complex wake structure than those species with prolate bells (Colin and Costello, 2002; McHenry and Jed, 2003). During the relaxation phase of the swimming cycle where the bell expands passively, a second vortex, known as a stopping vortex, is formed. The stopping vortex has opposite rotational direction to the starting vortex (created during bell contraction) and acts to refill the bell. The stopping vortices initially form on the outside of the bell but are repositioned by the flexible bell margin to the subumbrella cavity during bell expansion.

School of Biomedical Sciences, Faculty of Biological Sciences, University of Leeds, Leeds LS2 9JT, UK.
*Present address: School of Biological Sciences, University of Bristol, Bristol BS8 1TQ, UK.

‡Author for correspondence (g.n.askew@leeds.ac.uk)

T.R.N., 0000-0001-7536-3373; G.N.A., 0000-0003-1010-4439

Received 22 August 2018; Accepted 14 October 2018

Journal of Experimental Biology (2018) 221, jeb191148. doi:10.1242/jeb.191148

This increases the pressure in the subumbrella cavity, resulting in thrust generation and forward movement of the medusa. This passive energy recapture reduces the metabolic cost of locomotion in moon jellyfish (*Aurelia aurita*) by ∼48% (Gemmell et al., 2013).

The aims of this study were to determine the thrust-producing mechanisms and propulsive efficiency of the blue blubber jellyfish (*Catostylus mosaicus*, Quoy and Gaimard, 1824; order Rhizostomeae) by quantifying the wake structure during swimming. This species has a body morphology quite unlike that of any species studied to date: it lacks tentacles, instead possessing four oral lobes that converge over a central mouth, with eight branching oral arms that transport food to the mouth via a canal-like system (Lee et al., 2008). The feeding structures in *C. mosaicus* represent a much larger proportion of the overall body mass of the organism compared with many other species (Daniel, 1985; Arai, 1997). The bell of *C. mosaicus* is almost spherical in shape, with a bell height that is ∼60% of the bell diameter. Therefore, while still considered to be an oblate species, *C. mosaicus* has a morphology that is intermediate between that of typical prolate and oblate species. Additionally, *C. mosaicus* is a more active species than those that have previously been studied, with a relatively high pulsing frequency of ∼2–3 Hz. We hypothesised that the intermediate body morphology and large feeding structures of *C. mosaicus* would affect the formation of vortex structures and their interactions with one another during swimming in comparison to predominantly oblate and prolate medusae. Additionally, we hypothesised that the high pulsing frequency of *C. mosaicus* would result in closely spaced vortex rings, potentially providing a benefit in swimming performance to the animal during locomotion. In order to test these hypotheses, we measured the wake structure and propulsive efficiency in these animals during swimming.

MATERIALS AND METHODS

Animals

Blue blubber jellyfish (*Catostylus mosaicus* Quoy and Gaimard 1824) (Glass Ocean Ltd., London, UK) were housed in a 250 litre kreisel aquarium in artificial seawater (Instant Ocean, Aquarium Systems, Mentor, OH, USA). The aquarium was maintained at a temperature of 25°C and a salinity of 33 ppt, corresponding to conditions that the jellyfish would experience in their native habitat in the tropical waters of the Indian and Pacific Oceans (Southcott, 1982). Jellyfish were fed daily with freshly hatched brine shrimp. Relaxed bell diameter of the jellyfish ranged from 2.3 to 4.6 cm (mean±s.d.: 3.5±0.35). Jellyfish were allowed to acclimate to the laboratory conditions for a minimum of 1 week before the experiments took place.

Wake visualisation and analysis

Quantitative jet structure of the jellyfish was obtained using two-dimensional particle image velocimetry (PIV). PIV experiments took place in a 126 litre (610×460×450 mm) glass aquarium. The temperature and salinity of the experimental aquarium matched that of the holding tank. Individual jellyfish were transferred to the experimental tank and allowed to acclimatise for a minimum period of 15 min. Recordings took place once the jellyfish was actively swimming around the experimental aquarium.

The experimental tank was seeded with fine white talcum powder with a mean particle diameter of 26 µm at a density of 50 mg l^{-1} (Gilbert et al., 2018; Wong et al., 2012). Particles were illuminated with a 1 W continuous green (532 nm) laser (Shanghai Dream Lasers Technology Co., Ltd., Shanghai, People's Republic of China) directed through a Powell lens (Thorlabs, Inc., Newton, NJ, USA) creating a vertically oriented 1-mm-thick light sheet. The wake of swimming jellyfish was visualised in the vertical plane, with the light sheet oriented to bisect the animal and thus the jet. Only those sequences in which the laser crossed the central, vertical axis of the bell were used for analysis. The jellyfish and wake were recorded using a high-speed camera (Fastcam SA3, Photron USA, San Diego, USA) operating at 500 frames s^{-1}, shuttered at 1/500 s and recorded at 1024×1024 pixel resolution. The spatial resolution of the images was ∼0.4 mm $pixel^{-1}$. The particle image size was ∼1.5 pixels.

Fluid movements were determined by tracking the illuminated particles (PIVlab for MATLAB v.1.41; Thielicke and Stamhuis, 2014). The image sequences were pre-processed using the PIVlab contrast-limited adaptive histogram equalisation tool to enhance contrast and facilitate particle detection. The body of the jellyfish was masked on the images to eliminate edge effects. A cross correlation technique with adaptive, multi-pass processing was used to analyse image pairs and track particle movement between frames. A total of three passes were used to analyse images, with an initial interrogation window of 64×64 pixels and a final size of 16×16 pixels with a 50% overlap between each pass. A standard deviation filter was used to remove vectors more than 7 deviations away from the mean flow of the jet structures. An average of 0.68±0.03% (mean±s.e.m.) of the vectors were found to be erroneous across all swimming sequences. Missing velocity vectors were interpolated using a boundary value solver, which gives a smooth interpolation that tends towards the average boundary velocities. Pixel displacement within the jet structures ranged from 1 to 6 pixels during the jetting sequence.

The resultant sequences of particle motion were used to characterise the jet structures produced during swimming. Maximum vorticity was taken as the peak vorticity reached by the vortex rings over the entire swim cycle (where each swimming cycle is defined to be the period from the start of one bell contraction to the start of the next bell contraction). The average propulsive force ($\mathbf{F}_P$) was calculated by dividing the accumulated momentum (I) by the duration of the propulsion phase of the swim cycle (t_j), taken as the period from the beginning of bell contraction to the beginning of bell relaxation (Stamhuis and Nauwelaerts, 2005):

$$\mathbf{F}_P = \frac{I}{t_j} = \frac{\rho\Gamma\pi r^2}{t_j}, \quad (1)$$

where ρ is seawater density (1023 kg m^{-3}), r is the vortex ring radius and Γ is the circulation, calculated by integrating tangential velocity of a path around the vortex.

Swimming kinematics and whole cycle propulsive efficiency

Swimming kinematics were determined by tracking the position of the apex of the bell (Hedrick, 2008). Bell diameter over the course of the swimming cycle was determined from the positions of the extreme anterior and posterior edges of the bell margin. In order to calculate instantaneous swimming speed and body acceleration over the course of a swim (i.e. several bell contractions), 2D-positional data were filtered to reduce noise in the data, using a conservative cut-off frequency to avoid removing signal from the unfiltered data (following Bomphrey et al., 2009). The positional data were smoothed by fitting a quintic spline to the data, and the horizontal ($\mathbf{v}_x$) and vertical ($\mathbf{v}_y$) components of bell velocity were calculated as the first derivative of the horizontal (x) and vertical (y) position data,

Journal of Experimental Biology (2018) 221, jeb191148. doi:10.1242/jeb.191148

respectively. The instantaneous swimming speed of the jellyfish (U) was calculated as:

$$U = \sqrt{\mathbf{v}_x^2 + \mathbf{v}_y^2}. \quad (2)$$

Whole cycle propulsive efficiency (η_{wc}), the ratio of useful power to total power (i.e. the sum of useful and wasted power), was calculated using a method developed for jet propulsion swimming, and accounts for the acceleration of the water during both the refilling (intake) and contraction (expulsion) phases of the swimming cycle and is appropriate for animals with a rearward facing jet intake (Alexander, 2003; Neil and Askew, 2018):

$$\eta_{WC} = \frac{2\bar{U}\bar{u}_j}{2\bar{U}\bar{u}_j + \bar{u}_r^2 + \bar{u}_j^2}, \quad (3)$$

where $\bar{u}_j$ is the time-averaged jet velocity in the wake, $\bar{u}_r$ is time-averaged refill velocity of fluid into the bell and $\bar{U}$ is the time-averaged swimming speed of the jellyfish.

Statistical analyses

Statistical analysis was carried out in SPSS for Mac (IBM SPSS Statistics for Mac, v. 21.0, Armonk, NY, USA). Data were checked for normality using a Shapiro–Wilk test, *t*-tests were used to compare means. All data are reported as means±s.e.m.

RESULTS

The average swimming speed of the jellyfish was 36.22±1.22 mm s^{-1} and the average change in diameter of the bell margin during swimming was 8.1±0.90 mm, giving average Reynolds number and Strouhal numbers of 1184±220 and 0.25±0.12, respectively.

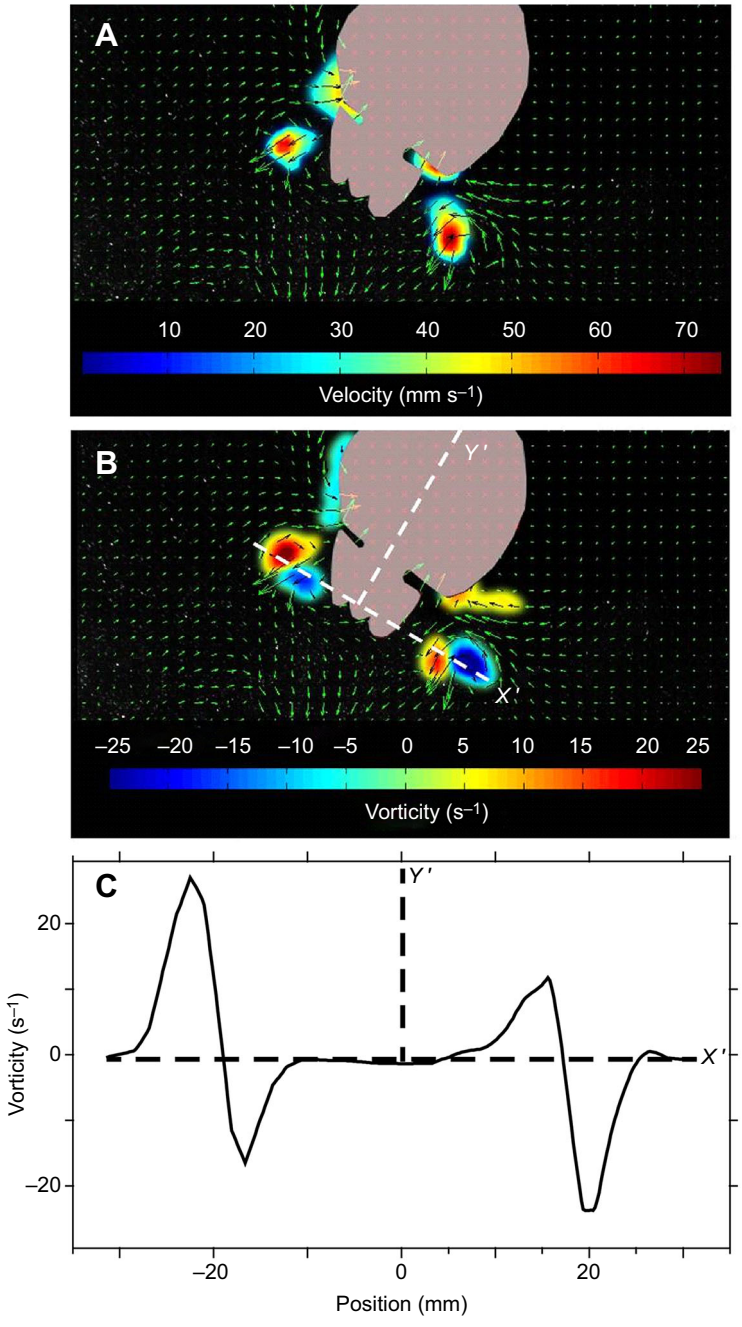

Fig. 1. Typical instantaneous flow and vorticity during free swimming in *Catostylus mosaicus*. (A) Instantaneous flow and (B) vortex ring vorticity distribution across a planar section through the wake of a swimming jellyfish; red and blue regions denote clockwise and counter-clockwise rotation, respectively. (C) Spatial distribution of vorticity distribution along the axis that transects the centres of fluid rotation of both vortex cores of the vortex rings (i.e. *X′* axis in B).

Journal of Experimental Biology (2018) 221, jeb191148. doi:10.1242/jeb.191148

The wake structure of swimming *C. mosaicus*

In total, 74 bouts of swimming from 5 individual medusae were analysed. The typical structure of the wake during swimming is shown in Fig. 1. During swimming, a series of vortices were produced. Upon bell contraction, a starting vortex was generated at the bell margin (Fig. 2D). At the same time, the stopping vortex produced in the preceding contraction cycle, was ejected out of the subumbrella cavity. The pair of counter-rotating vortex rings interact, creating a jet of fluid in between (Fig. 1), and forming a downstream vortex superstructure (Fig. 2D,E). The vorticity distributions of the shed vortices in the animal's wake (Fig. 1C) are typical of a vortex ring (see Gharib et al., 1998), and indicate the vorticity of the starting vortex and the shed part of the stopping vortex on each side of the swimming medusa.

The sequential shedding of the stopping vortex followed by starting vortex, resulted in the starting vortex being located more laterally and closer to the oral surface than the stopping vortex. Therefore, the resulting jet was orientated at an angle of 26.0± 2.2 deg (range=13.3 to 42.6 deg) to the mid-line of the jellyfish (Y'-axis in Fig. 1B).

In addition to the fluid that is ejected during bell contraction, these jellyfish also created vortices through the movements of their bell margin, which acts like a paddle as the jellyfish 'rows' through the water. The formation of these vortices started during bell relaxation, with fluid rolling up over the top of the bell as the bell expanded and created a stopping vortex (Fig. 2A). The movement of the bell and extension of the bell margin, led to the stopping vortex being repositioned under the jellyfish, resulting in a flow of water into the subumbrella cavity (Fig. 2C). The bell margin moved under the jellyfish during the initial stage of relaxation (Fig. 3), increasing fluid circulation in the stopping vortex. The stopping vortices that are created during bell expansion exhibit significantly higher circulation than the starting vortices (over the swimming cycle, starting vortex circulation is 1.90±0.35 m^2 s^{-1} and stopping vortex circulation is 5.50±1.06 m^2 s^{-1}; $t_{1,4}$=−3.206, P<0.05). There was no significant difference in the size of the stopping and starting vortices (starting vortex radius is 1.94±0.32 cm whilst the stopping

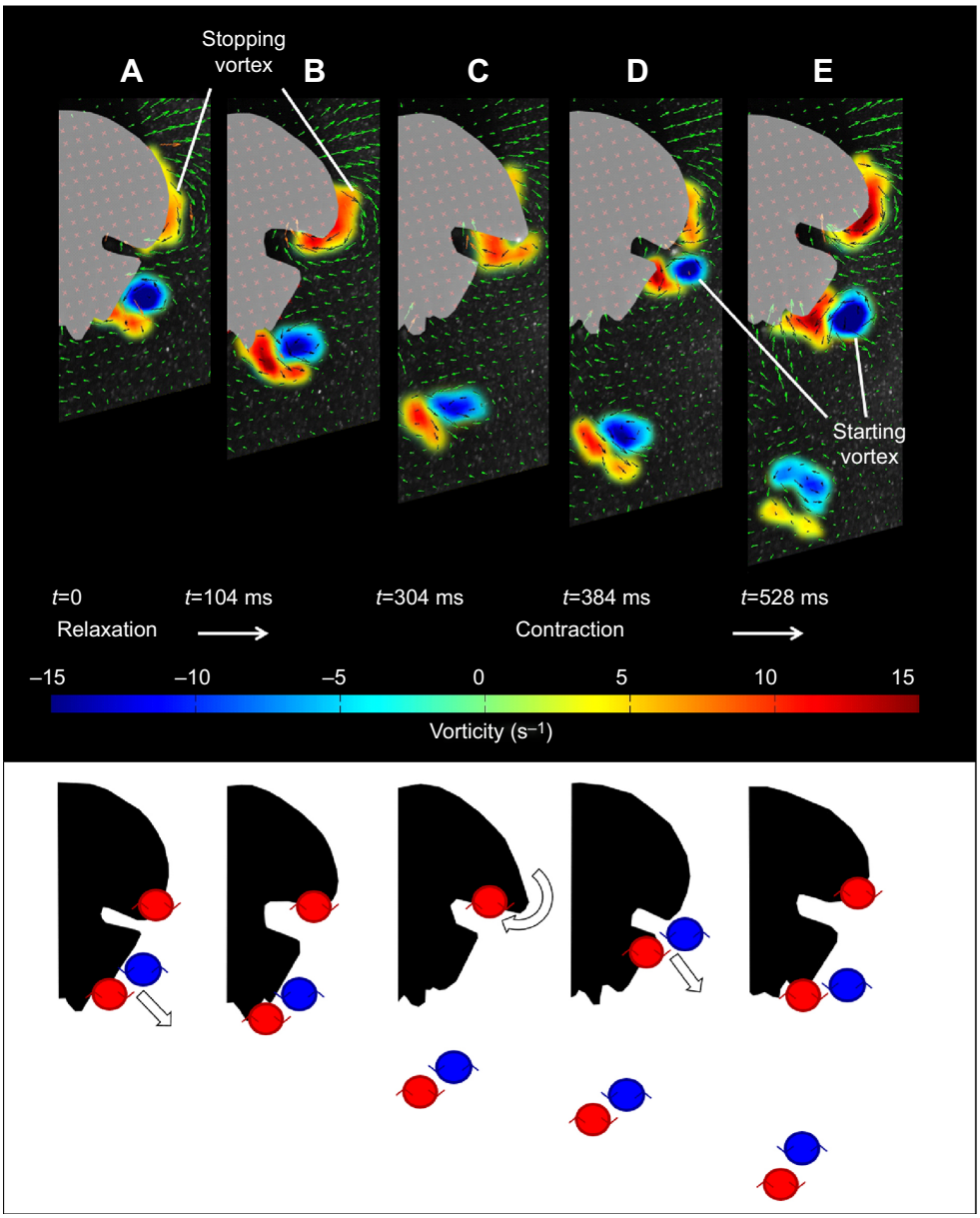

Fig. 2. Formation and development of stopping and starting vortices during swimming in *C. mosaicus*. At the beginning of the relaxation phase of the swimming cycle, the stopping vortex forms on the outside edge of the bell margin but has low vorticity. (B) Expansion of the bell coupled with extension of the bell margin increases vorticity. (C) At the end of the relaxation phase, the vortex ring has been repositioned into the subumbrella cavity of the jellyfish. (D) At the beginning of contraction, part of the stopping vortex is ejected from the subumbrella cavity and interacts with the starting vortex that has formed at the bell margin. (E) The vortices move away from the jellyfish as a vortex superstructure. Red and blue regions denote clockwise and counter clockwise rotation, respectively. Vortices are simplified in cartoon below each panel; large arrows indicate the direction of fluid flow during the swimming cycle. See also Movie 1, which shows *C. mosaicus* swimming through a sheet of illuminated particles and the sequential shedding of counter-rotating vortices.

Journal of Experimental Biology (2018) 221, jeb191148. doi:10.1242/jeb.191148

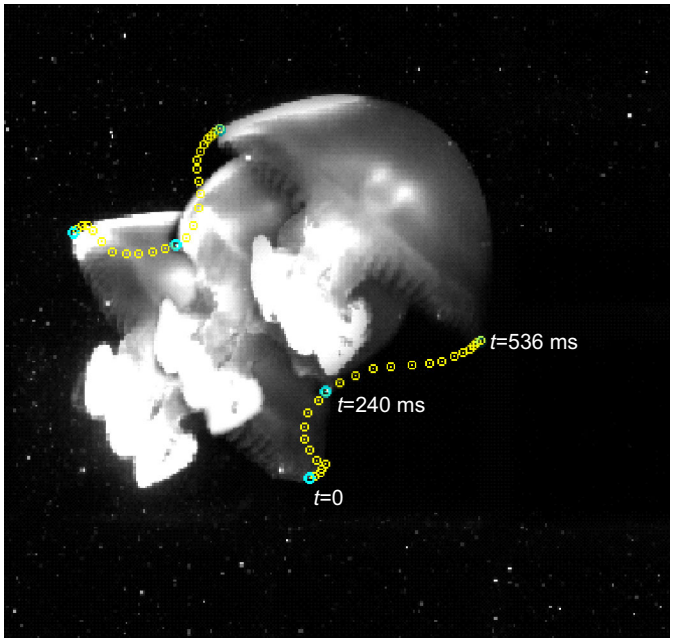

Fig. 3. Kinematics of *C. mosaicus* over one bell contraction cycle. The body is imaged at the start (0 ms), middle (240 ms) and end (536 ms) of bell contraction. The trajectory of the bell margin is indicated using yellow and blue (corresponding to the indicated times) symbols.

vortex radius is 1.75±0.27 cm; $t_{1,4}$=0.432, P=0.68). As thrust is directly proportional to vorticity, the stopping vortex (with vorticity enhanced by the movements of the bell margin) created additional thrust contributing to the propulsion of the animal. The mean thrust produced by the stopping vortices was significantly higher than that produced by the starting vortices (stopping vortex: 2.62±1.00 mN; starting vortex 1.38±0.47 mN; $t_{1,4}$=2.591, P<0.05).

The spacing between the sequentially shed vortices ranged from 2.4 to 10.5 vortex ring radii (4.65±0.64 radii). There was no significant difference in thrust produced in swimming bouts where vortex rings were less than 3 radii apart compared with when the spacing exceeded 3 radii ($t_{1,4}$=1.358, P=0.212).

Swimming kinematics

Average swimming speed of *C. mosaicus* was 36.22±1.22 mm s^{-1}, whereas mean contraction frequency was 2.18±0.05 Hz. The contraction phase represented 0.34±0.01 of the total contraction cycle (i.e. duty cycle). The swimming speed of *C. mosaicus* fluctuated over the course of a swimming cycle, increasing rapidly following the onset of the contraction phase of the cycle, and reaching peak speed at the end of bell contraction phase when the bell diameter was smallest (Fig. 4). Swimming speed decreased (but the animal continued to move forwards) during bell relaxation, reaching a minimum as the bell approached maximum expansion (Fig. 4). The distance covered during the post relaxation phase is, on average, 11.44±1.02% of the total distance covered during one swim cycle. An average of 37.08±1.51% of the distance travelled by *C. mosaicus* during one swimming cycle was covered in the relaxation phase of the cycle, whereas 51.49±1.53% occurs during bell contraction. Mean whole cycle efficiency was 0.51±0.15.

DISCUSSION

Previous work has suggested that there is a trade-off between swimming performance and swimming efficiency in medusae that swim by jet propulsion (Dabiri et al., 2010), with more oblate cruising species swimming with greater efficiencies but lower absolute speeds than those with a more prolate body shape. Like other jellyfish, *C. mosaicus* swims by jet propulsion; however, this species has an unusual morphology with relatively large feeding structures compared with many other species. It was hypothesised that these feeding structures might affect the mechanisms by which thrust is produced in this species, and thus their swimming efficiency.

The wake structures observed in swimming *C. mosaicus* shared several similarities of those structures observed in other oblate medusae that use a rowing mode of jet propulsion. The formation of a stopping vortex during bell expansion has previously been observed in another species of oblate medusa (*A. aurita*; Dabiri et al., 2005; Gemmell et al., 2013) but is absent in prolate medusae (Dabiri et al., 2010). However, the dynamics of the interaction between the stopping and starting vortices, differs between *C. mosaicus* and *A. aurita*. In *A. aurita* the stopping vortex that is formed during the expansion phase of the swimming cycle, persists in the subumbrella cavity following the end of relaxation, and then contributes to the formation of the subsequent starting vortex. The two vortices interact as they move downstream in the wake, resulting in the starting vortex growing in volume but decreasing in circulation, as they have oppositely signed vorticities. Despite this, there is still a net gain in momentum of each wake vortex, as the increased mass of the associated interaction outweighs the loss of circulation due to vorticity cancellation. The shed vortices of *C. mosaicus* are similar to those in *A. aurita* in the sense that the starting vortex does interact with the stopping vortex of the proceeding swim cycle and contributes to the wake produced during the power stroke of the cycle. However, in *C. mosaicus*, the starting vortex is created in close proximity to the stopping vortex that has formed in the subumbrella cavity. During bell contraction, these vortices of opposite rotation move ventrally, away from the medusa in the wake in such a way that a jet of fluid with a high velocity is created along the line of interaction, producing a thrust force that propels the jellyfish forward. The sequential shedding of the stopping followed by starting vortex in *C. mosaicus*, results in the starting vortex being located more laterally and closer to the oral surface than the stopping vortex during swimming; the thrust force is therefore generated at an angle to the animal's path of motion. The jet structures observed in swimming *C. mosaicus* and the interactions between the starting and stopping vortices are consistent with predictions of computational fluid dynamic models of the rowing oblate medusa *Aequorea victoria* (Sahin et al., 2009).

In *C. mosaicus* it is apparent that the flexible bell margin plays a role in the modulation of the fluid movements that results in thrust, via two different mechanisms. During the initial stages of bell expansion, the pressure in the subumbrellar cavity is low as refilling occurs; subsequently, however, the flexible bell margin moves in such a way that the stopping vortex moves around the bell margin of the medusa (Fig. 2B) and is repositioned underneath the subumbrellar cavity. In *A. aurita*, this creates positive pressure within the subumbrellar cavity and sufficient force to produce a secondary peak in velocity towards the end of bell expansion (Gemmell et al., 2015). We propose that the positive acceleration peak in *C. mosaicus* that coincides with peak bell diameter is the result of a similar build-up of high pressure that follows the repositioning of the stopping vortex into the subumbrellar cavity (Fig. 2D). Computational approaches have additionally predicted that as the bell margin tucks underneath the subumbrellar cavity (t=240 ms, Fig. 3), a region of low pressure is created on the inner surface of the bell margin (see fig. 9D in Sahin et al., 2009),

Journal of Experimental Biology (2018) 221, jeb191148. doi:10.1242/jeb.191148

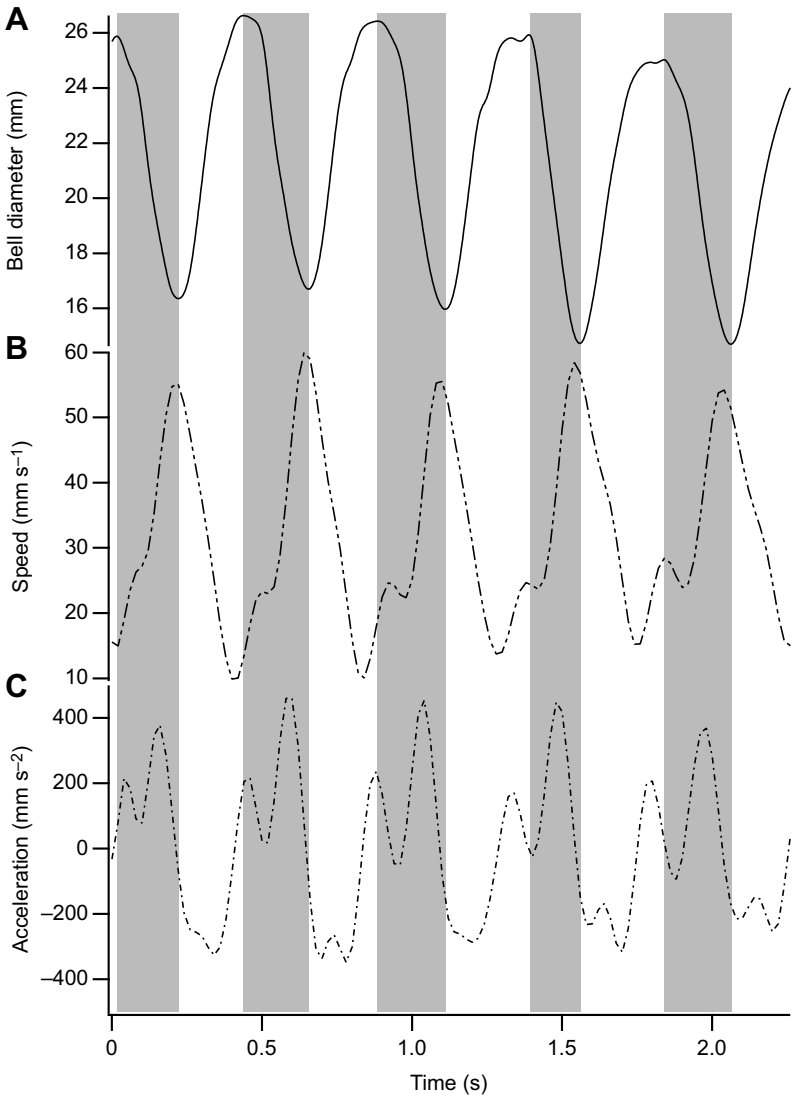

Fig. 4. Speed and acceleration in relation to movements of the bell during swimming in *C. mosaicus*. (A) Bell diameter, (B) swimming speed and (C) acceleration are illustrated over five bell contraction cycles. Raw positional data for this particular swim were filtered using a cut-off frequency of 8 Hz (for both *x* and *y* data) and smoothed using a quantic spline (see Materials and Methods for details). Grey shading indicates the contraction phase and white areas indicate the relaxation phase of the swimming cycle.

orientated in the direction of travel, which creates thrust (Sahin et al., 2009). This may be the mechanism underlying the peak in force during bell expansion (Gemmell et al., 2013) and that consequently reduces the deceleration of *C. mosaicus* approximately half-way through bell expansion (Fig. 4C).

As the refilling of the bell is powered entirely from the release of elastic energy stored in the mesoglea (DeMont and Gosline, 1988), it has been suggested that this is a mechanism for increasing swimming efficiency by reducing the metabolic cost of swimming (potentially by 48% in *A. aurita*; Gemmell et al., 2013). However, the higher cycle frequency in *C. mosaicus* and the shorter duration of the relaxation phase may reduce the propulsion obtained before the onset of the next contraction cycle in this species. In *A. aurita*, ∼32% of the total distance travelled in a swim cycle occurs during this post-relaxation phase (Gemmell et al., 2013), whereas in *C. mosaicus*, the distance travelled in this phase is only ∼11% of the total distance covered.

In *A. aurita* (Dabiri et al., 2005), successive vortex rings interact, inducing flow of fluid toward the central axis of the medusa, and indicating that thrust may be enhanced, as suggested previously (Weihs, 1977). During swimming in *C. mosaicus*, vortex ring separation ranged from 2.4 to 10.5 radii between rings, covering the range of within 3 ring radii that Weihs predicted would increase thrust generation (Weihs, 1977). However, there was no significant difference in thrust produced in swimming bouts where vortex rings were less than 3 radii apart compared with when the spacing exceeded 3 radii (*t*-test; $t=-0.111$; d.f.=70; $P>0.05$), indicating that thrust is not enhanced by induced flow between adjacent vortex rings. Despite predictions that vortex rings within 3 radii might offer some kind of thrust augmentation, in *A. aurita* it was found that vortices had to be much closer than this for any benefit to be observed, with vortices in *A. aurita* being between 1–1.4 radii apart (Dabiri et al., 2005). Discrepancies between predicted and empirical measurements may be due to the fact that Weihs based his models on fully pulsed jets, not the jet-paddle mode of swimming observed in *C. mosaicus*, leading to differences in how individual vortices interact with one another once they have left the jellyfish in the wake (Weihs, 1977). Indeed, there was no sign of induced flows between vortex rings during swimming in *C. mosaicus*.

Swimming efficiency

The hydrodynamic efficiency in *C. mosaicus* was relatively high 0.53 (±0.10), compared with the range measured in other medusae (0.09–0.53; Dabiri et al., 2010). The swimming efficiency is comparable to values measured in other jet propulsion swimmers such as salps (0.47–0.55; Sutherland and Madin, 2010), squid

(0.42–0.49; Anderson and Grosenbaugh, 2005) and *Nautilus* (0.36–0.76; Neil and Askew, 2018).

Potential impact of the wake on feeding

The structure of the wake is likely to play an important role in feeding for *C. mosaicus*. Studies on other jellyfish species have suggested that increased fluid mixing at the oral arms increases the likelihood of food or prey coming into contact with the feeding tentacles and improving the rate of prey capture (Dabiri et al., 2005). In the case of *C. mosaicus*, the interaction between stopping and starting vortices results in a mass of fluid that travels down through the oral arms as the vortex rings move away from the medusa in the wake. Similar fluid movements, with counter-rotating vortices emanating from the subumbrella cavity and passing down towards the oral arms, have been reported in the upside-down jellyfish *Cassiopea xamachana* (Hamlet et al., 2011), although the mode of foraging differs between the two species. Instead of actively swimming like *C. mosaicus*, *C. xamachana* spends most of its time upside down on the sea floor, using bell pulsations to pass water over its oral arms to facilitate feeding. The similarities in body morphology and wake dynamics suggest that despite differences in foraging ecology, comparable strategies are employed.

Conclusions

The ability of *C. mosaicus* to rapidly form enormous population blooms (bloom biomass can exceed 500 tonnes km^{-2}; Pitt and Kingsford, 2003) in the tropical estuaries and coastal waters of the Indian and Pacific Oceans (Gibson and Barnes, 2003) and take over disturbed environments is at odds with the general perception that animals that swim by jet propulsion are energetically inefficient. However, we show here that the generation of a vortex superstructure through the interaction between stopping and starting vortices, and passive energy recapture during bell expansion results in *C. mosaicus* having a relatively high propulsive efficiency compared with other swimmers, including the medusae of some other species of jellyfish. Economical locomotion in *C. mosaicus* could be a contributing factor in the ecological success of these medusan swimmers.

Acknowledgements

The authors thank Dr Simon Walker for assisting us in filtering and smoothing position data.

Competing interests

The authors declare no competing or financial interests.

Author contributions

Conceptualization: T.N., G.N.A.; Methodology: T.N., G.N.A.; Formal analysis: T.N., G.N.A.; Investigation: T.N., G.N.A.; Resources: G.N.A.; Data curation: G.N.A.; Writing - original draft: T.N.; Writing - review & editing: T.N., G.N.A.; Supervision: G.N.A.; Project administration: G.N.A.; Funding acquisition: G.N.A.

Funding

This work was funded by an Engineering and Physical Sciences Research Council (EPSRC, EP/K503526/1) UK Institutional sponsorship grant.

Data availability

Supporting data are available in the Research Data Leeds Repository: https://doi.org/10.5518/460

Supplementary information

Supplementary information available online at
http://jeb.biologists.org/lookup/doi/10.1242/jeb.175281.supplemental

References

Alexander, R. M. (2003). *Principles of Animal Locomotion*. Princeton University Press.

Anderson, E. J. and Grosenbaugh, M. A. (2005). Jet flow in steadily swimming adult squid. *J. Exp. Biol.* **208**, 1125-1146.

Arai, M. N. (1997). *A Functional Biology of Scyphozoa*. Springer Science & Business Media.

Bomphrey, R. J., Walker, S. M. and Taylor, G. K. (2009). The typical flight performance of blowflies: measuring the normal performance envelope of *Calliphora vicina* using a novel corner-cube arena. *PLoS ONE* **4**, e7852.

Colin, S. P. and Costello, J. H. (2002). Morphology, swimming performance and propulsive mode of six co-occurring hydromedusae. *J. Exp. Biol.* **205**, 427-437.

Dabiri, J. O. and Gharib, M. (2004). Delay of vortex ring pinchoff by an imposed bulk counterflow. *Phys. Fluids* **16**, L28-L30.

Dabiri, J. O., Colin, S. P., Costello, J. H. and Gharib, M. (2005). Flow patterns generated by oblate medusan jellyfish: field measurements and laboratory analyses. *J. Exp. Biol.* **208**, 1257-1265.

Dabiri, J. O., Colin, S. P., Katija, K. and Costello, J. H. (2010). A wake-based correlate of swimming performance and foraging behavior in seven co-occurring jellyfish species. *J. Exp. Biol.* **213**, 1217-1225.

Daniel, T. L. (1985). Cost of locomotion: unsteady medusan swimming. *J. Exp. Biol.* **119**, 149-164.

DeMont, M. E. and Gosline, J. M. (1988). Mechanics of jet propulsion in the hydromedusan jellyfish, *Polyorchis pexicillatus*: I. Mechanical properties of the locomotor structure. *J. Exp. Biol.* **134**, 313-332.

Gemmell, B. J., Costello, J. H., Colin, S. P., Stewart, C. J., Dabiri, J. O., Tafti, D. and Priya, S. (2013). Passive energy recapture in jellyfish contributes to propulsive advantage over other metazoans. *Proc. Natl. Acad. Sci. USA* **44**, 17904-17909.

Gemmell, B. J., Troolin, D. R., Costello, J. H., Colin, S. P. and Satterlie, R. A. (2015). Control of vortex rings for manoeuvrability. *J. R. Soc. Interface* **12**, 20150389.

Gharib, M., Rambod, E. and Shariff, K. (1998). A universal time scale for vortex ring formation. *J. Fluid Mech.* **360**, 121-140.

Gibson, R. N. and Barnes, M. (2003). Management of jellyfish fisheries, with special reference to the order Rhizostomeae. In *Oceanography and Marine Biology: An Annual Review*, Vol. 38, pp. 85-156. CRC Press.

Gilbert, C. R., Furman, B. R., Feller-Kopman, D. J. and Haouzi, P. (2018). Description of particle size, distribution, and behavior of talc preparations commercially available within the United States. *J. Bronchol. Interv. Pulmonol.* **25**, 25-30.

Hamlet, C., Santhanakrishnan, A. and Miller, L. A. (2011). A numerical study of the effects of bell pulsation dynamics and oral arms on the exchange currents generated by the upside-down jellyfish *Cassiopea xamachana*. *J. Exp. Biol.* **214**, 1911-1921.

Hedrick, T. L. (2008). Software techniques for two-and three-dimensional kinematic measurements of biological and biomimetic systems. *Bioinspir. Biomim.* **3**, 034001.

Lee, H. E., Yoon, W. D. and Lim, D. (2008). Description of feeding apparatus and mechanism in *Nemopilema nomurai* kishinouye (Scyphozoa: Rhizostomeae). *Ocean Sci. J.* **43**, 61-65.

McHenry, M. J. and Jed, J. (2003). The ontogenetic scaling of hydrodynamics and swimming performance in jellyfish (*Aurelia aurita*). *J. Exp. Biol.* **206**, 4125-4137.

Neil, T. R. and Askew, G. N. (2018). Swimming mechanics and propulsive efficiency in the chambered nautilus. *R. Soc. Open Sci.* **5**, 170467.

Pitt, K. A. and Kingsford, M. J. (2003). Temporal variation in the virgin biomass of the edible jellyfish, *Catostylus mosaicus* (Scyphozoa, Rhizostomeae). *Fish. Res.* **63**, 303-313.

Quoy, J. R. C. and Gaimard, P. (1824). *Zoologie*. Imprimerie Royale.

Sahin, M., Mohseni, K. and Colin, S. P. (2009). The numerical comparison of flow patterns and propulsive performances for the hydromedusae *Sarsia tubulosa* and *Aequorea victoria*. *J. Exp. Biol.* **212**, 2656-2667.

Southcott, R. (1982). Jellyfishes (Classes Scyphozoa and Hydrozoa). *Mar. Invertebr. South. Aust. Part I*, 115-159.

Stamhuis, E. J. and Nauwelaerts, S. (2005). Propulsive force calculations in swimming frogs II. Application of a vortex ring model to DPIV data. *J. Exp. Biol.* **208**, 1445-1451.

Sutherland, K. R. and Madin, L. P. (2010). Comparative jet wake structure and swimming performance of salps. *J. Exp. Biol.* **213**, 2967-2975.

Thielicke, W. and Stamhuis, E. J. (2014). PIVlab – towards user-friendly, affordable and accurate digital particle image velocimetry in MATLAB. *J. Open Res. Soft.* **2**, p.e30.

Weihs, D. (1977). Periodic jet propulsion of aquatic creatures. *Forsch. Zool.* **24**, 171-175.

Weston, J., Colin, S. P., Costello, J. H. and Abbott, E. (2009). Changing form and function during development in rowing hydromedusae. *Mar. Ecol. Prog. Ser.* **374**, 127-134.

Wong, C. Y., Nathan, G. J. and Kelso, R. M. (2012). PIV as a complement to LDA in the study of an unsteady oscillating turbulent flow. In *The Particle Image Velocimetry* (ed. G. Cavazzini). *IntechOpen*, doi: 10.5772/34696. Available from: https://www.intechopen.com/books/the-particle-image-velocimetry-characteristics-limits-and-possible-applications/piv-as-a-complement-to-lda-in-the-study-of-an-unsteady-oscillating-turbulent-flow.